

# Search of the proper extraction method of CME leading edges from several satellite coronagraph images registered during the last solar cycle

*Zbigniew Kobylinski, Jerzy Bialy, Tomasz Seredyn*

Polish Air Force Academy, Deblin, Poland

## **Abstract**

The standard procedure of the detection and tracking of the CMEs from the middle to the outer corona is the visual valuation and then preparing height – time profiles of the CMEs. The CMEs height at any given instant is calculated from the outermost point of the leading edge to the heliospheric center in the snapshots of CMEs images. Several attempts of CME images analyzing have been made in order to use in a system of automatic CME detection using digital image processing methods. Segmentation procedures are based on detecting sharp, local changes in intensity, generally there are three types of image features that could be extracted: isolated points, lines and edges. In this work, we compare the following edge detectors: Roberts, Prewitt, Sobel, LoG and Canny using them to analyze the two sequences of LASCO CMEs images from the period 2000 - 2003. We have exhibited LoG and Canny as the best detectors for extraction of CME leading edges. After obtaining the front edges it is possible to study structure and evolution of CMEs in the broad spectrum of directions as it is seen from the showed images. We apply this technique to the CMEs observed on 18 Apr 2000 and 1 Jun 2003, by the Large Angle Solar Coronagraph experiment (LASCO) C2/C3. Obtained plots of height – time and values of mean velocities in every case are presented.

## 1. Introduction

Digital image processing consists of the following fundamental steps: image processing and segmentation, image representation and description, object recognition. Segmentation of image is one of the most difficult tasks in image processing. Segmentation procedures are based on detecting sharp, local changes in intensity. Generally, there are three types of image features that could be extracted: isolated points, lines and edges. Edge pixels are pixels which intensity of an image function changes abruptly, and edges are sets of connected edge pixels. [1]

The standard procedure of the detection and tracking of the CMEs evolution from the middle to the outer corona is the visual valuation and then preparing height – time profiles of the CMEs. The CMEs height at any given instant is calculated from the outermost point of the leading edge to the heliospheric center in the snapshots of CMEs images (e.g. CDAW CME catalog [2]). The LASCO Interactive Data Language is used for parameters calculation. Such methodology is subjective and depends on the individual features of the determined observer [3].

In the relation to CMEs images determining of the structure and edges of such solar phenomena by means of digital segmentation is impeded by the fact, that CMEs are diffusive objects with ill-defined boundaries and the images from SOHO and TRACE are not distinct as e.g. photos prepared on the Earth. However, several attempts of CME images analyzing have been made in order to use in a system of automatic CME detection. We can mention here - combination of wavelet and gradient based techniques proposed by Young and Gallagher [4], wavelet based intensity contrast-enhancement technique (WISE) developed by Stenborg and Cobelli [5], wavelet multilevel decomposition used by Portier-Fozzani at al. [6], Hough transform employed to autonomously detecting of CMEs in image sequences from LASCO by means of the software Computer Aided CME Tracking (CACTus) [7] prepared by Robbrecht and Berghmans [8]. The last method has a limitation that it imposes a linear height – time evolution, therefore forcing constant velocity profiles, thus it is not appropriate to study CME acceleration.

In this work, we compare the following edge detectors: Roberts, Prewitt, Sobel, LoG and Canny using them to analyze the several sequences of LASCO CMEs images from the period 2001 - 2003. The best detectors for extracting of CME leading edge have been exhibited as LoG and Canny, but the last one is more sensitive for delicate changes of image local intensity, therefore in order to determine the high – time profiles, mean velocities and accelerations of investigated CMEs we have used Canny detector. Obtained leading edges by this method makes possible studying of the the structure and evolution of CMEs in the broad spectrum of directions as it is seen from the showed images. We apply this technique to the CMEs observed on: 18 April 2000 and 1 June 2003 by the Large Angle Solar Coronagraph experiment (LASCO) C2/C3. Obtained plots of height – time and values of mean velocities in every cases are presented quoting [9].

## 2. Edge detection methods used

There are three fundamental steps in the edge detection:

- 1) image smoothing for noise reduction
- 2) detection of points as potential fragments of edges
- 3) edge localization.

The majority of edge extraction methods is based on gradient or Laplacian operator of the image function  $f(x)$ .

Gradient  $f(x)$  in the point  $(x,y)$  is a 2-D vector which shows the direction of the biggest change

$$f = \text{grad } f = \begin{bmatrix} g_x \\ g_y \end{bmatrix} = \begin{bmatrix} \frac{\partial f}{\partial x} \\ \frac{\partial f}{\partial y} \end{bmatrix} \quad (1)$$

his length is equal  $M(x,y) = \sqrt{g_x^2 + g_y^2}$  (2)

A spatial filtering consists of 1) a neighborhood (typically a small rectangle) and 2) a predefined operation that is perfor-

med on the image pixels encompassed by the neighborhood.

On the figure a 3 x 3 region of an image called "mask" ( $f_i$  are intensity values):

$f_1$	$f_2$	$f_3$
$f_4$	$f_5$	$f_6$
$f_7$	$f_8$	$f_9$

and lower approximations of the partial derivatives are shown for the point  $(x_i, y_j)$  from neighborhood 3 x 3 accordingly to:

Roberts [10]

$$g_x = f_9 - f_5 \quad \text{and} \quad g_y = f_8 - f_4, \quad M(x,y) = [(f_9 - f_5)^2 + (f_8 - f_4)^2]^{1/2}, \quad (3)$$

Sobel [11]

$$g_x = (f_7 + 2 f_8 + f_9) - (f_1 + 2 f_2 + f_3) \quad \text{and} \quad g_y = (f_3 + 2 f_6 + f_9) - (f_1 + 2 f_4 + f_7), \quad (4)$$

Prewitt [12]

$$g_x = (f_7 + f_8 + f_9) - (f_1 + f_2 + f_3) \quad \text{and} \quad g_y = (f_3 + f_6 + f_9) - (f_1 + f_4 + f_7) \quad (5)$$

-1	0	0	-1
0	1	1	0

Roberts

-1	-2	-1
0	0	0
1	2	1

Sobel

-1	0	1
-2	0	2
-1	0	1

-1	-1	-1
0	0	0
1	1	1

Prewitt

-1	0	1
-1	0	1
-1	0	1

Laplacian  $\nabla^2 f(x)$ :

$$\nabla^2 f = \frac{\partial^2 f}{\partial x^2} + \frac{\partial^2 f}{\partial y^2} \quad (6)$$

and approximations of the second derivatives and examples of masks:

$$\frac{\partial^2 f}{\partial x^2} = f(x+1, y) + f(x-1, y) - 2f(x, y) \quad \frac{\partial^2 f}{\partial y^2} = f(x, y+1) + f(x, y-1) - 2f(x, y) \quad (7)$$

$$\nabla^2 f(x,y) = f(x+1, y) + f(x-1, y) + f(x, y+1) + f(x, y-1) - 4f(x, y) \quad (8)$$

0	1	0
1	-4	1
0	1	0

1	1	1
1	-8	1
1	1	1

0	-1	0
0	1	0
0	0	0

0	-1	0
0	1	0
0	0	0

The Marr-Hildreth edge detector [13], called also LoG filter is the filter  $\nabla^2 G$ , where  $G$  is the 2-D Gaussian function,  $\sigma$  is the standard deviation. The final expression is following:

$$\nabla^2 G = \left[ \frac{x^2 + y^2 - 2\sigma^2}{\sigma^4} \right] e^{-\frac{x^2+y^2}{2\sigma^2}} \quad (9)$$

The Marr-Hildreth algorithm consists of convolving the LoG filter with an input image,  $f(x,y)$ ,

$$g(x,y) = \nabla^2 G(x,y) * f(x,y) \quad (10)$$

and then finding the zero crossing of  $g(x,y)$  to determine the locatin of edges in  $f(x,y)$ .

The Canny edge detector is an edge detection operator that uses a multi-stage algorithm to detect a wide range of edges in images<sup>i/</sup>. The general criteria for edge detection includes

1. detection of edge with low error rate, which means that the detection should accurately catch as many edges shown in the image as possible
2. the edge point detected from the operator should accurately localize on the center of the edge.
3. a given edge in the image should only be marked once, and where possible, image noise should not create false edges.

The Process of Canny edge detection algorithm can be broken down to 5 different steps, and each of them is precisely described in: [14].

- 1) apply Gaussian filter to smooth the image in order to remove the noise,
- 2) find the intensity gradients of the image,
- 3) apply non-maximum suppression to get rid of spurious response to edge detection,
- 4) apply double threshold to determine potential edges,
- 5) track edge by hysteresis: finalize the detection of edges by suppressing all the other edges that are weak and not connected to strong edges.

### 3. The choice of the method

**Fig. 1.** Original images: CME 18 Apr 2000 from LASCO C2/C3 [15]

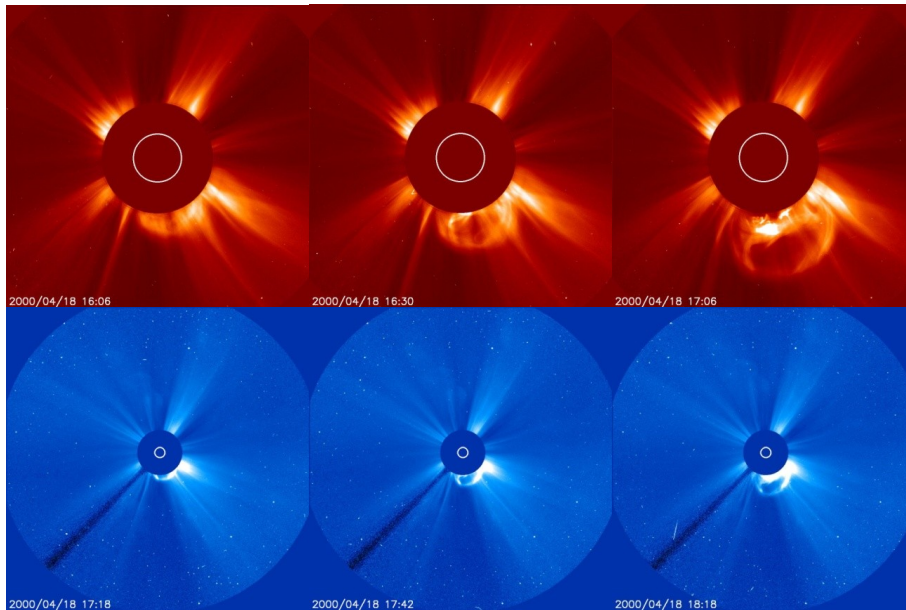


**Fig. 2.** Four images after smoothing of histogram and increasing of contrast by 20 for C2 and 30 for C3 in program GIMP [16]. CME is better visible. Lower panels: histograms.

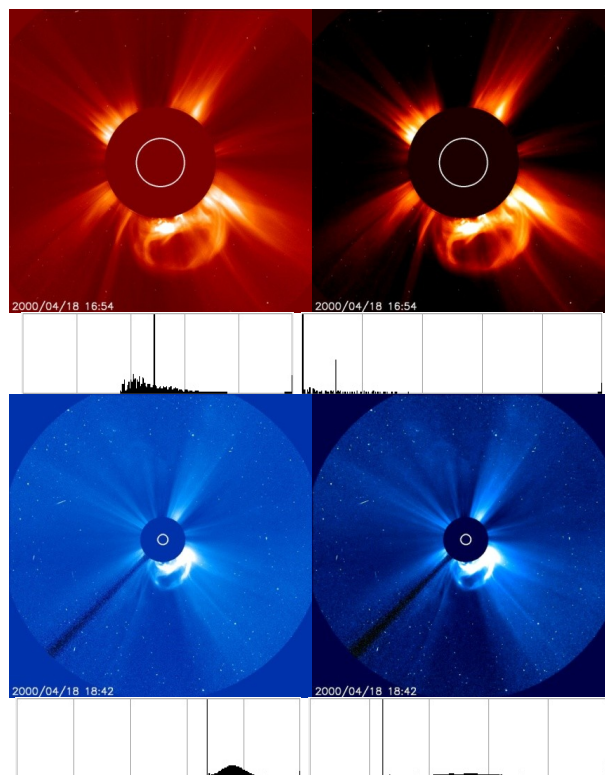
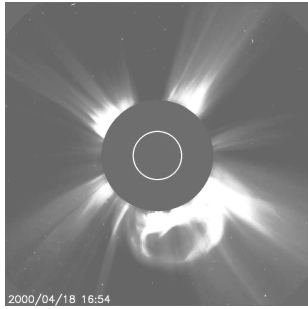


**Fig. 3.** Image from Fig. 2 (C2) have been divested of color in Matlab Image Toolbox and denoising by Wiener filter.



The next step: this image after filtration by mentioned methods. Parameters have been chosen experimentally. Matlab commands with the best values of parameters::

- Roberts - „R = edge (IS, 'roberts', 0.005);”
- Prewitt - „P = edge (IS, 'prewitt', 0.006);”
- Sobel “S = edge (IS, 'sobel', 0.005);”
- LoG “L = edge (IS, 'log', 0.00002, 5);”
- Canny - “L = edge (IS, 'canny', 0.01, 5);”

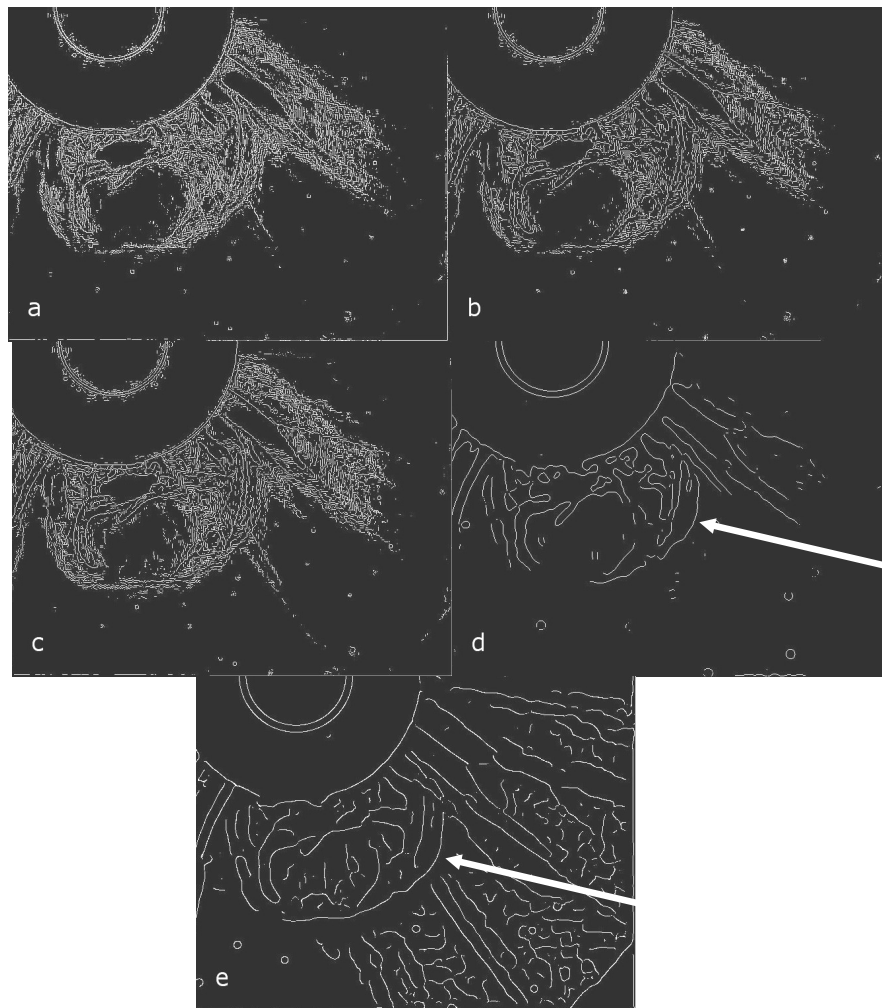


**Fig. 4.** Edge detection by means of: a) Roberts, b) Prewitt, c) Sobel, d) LoG, e) Canny, filters

The best result has been obtained with Canny method (4 e)- the leading edge has been well extracted (see arrows), LoG gives also the well determined leading edge but it has gaps.

Then, after a preparation of images: 4e and original one from Fig. 1, they have been put on for better visualization using GIMP, as it is seen on Figures 5 and 6.

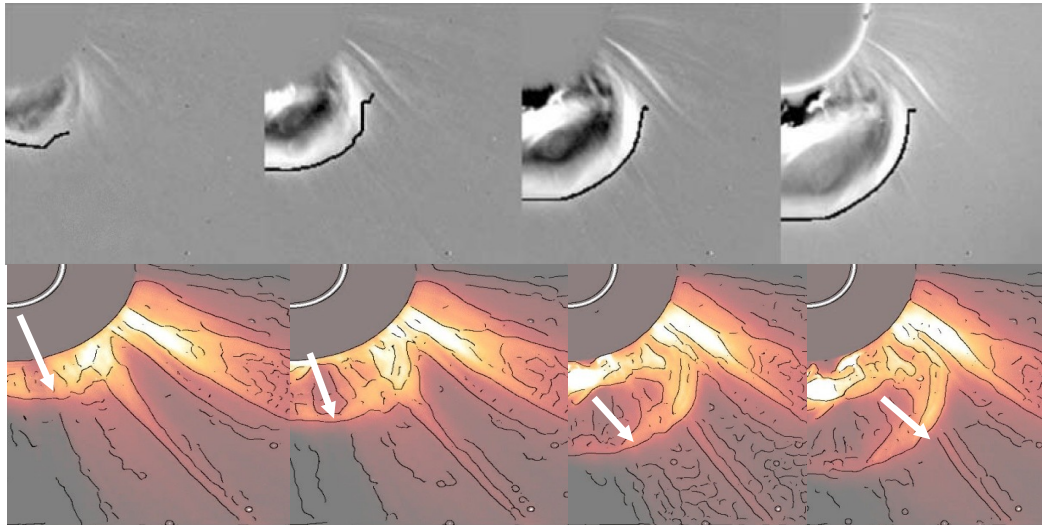


**Fig. 5.** The comparison of 4 LASCO C2 images – higher: after application of the multiscale edge detection by Young and Gallagher <sup>4/</sup>, lower: by means of Canny method described above, leading edges are shown by arrows. The times for these pictures (from left to right) 16:06 UT, 16:30 UT, 16:54 UT, 17:06 UT on 18 April 2000.

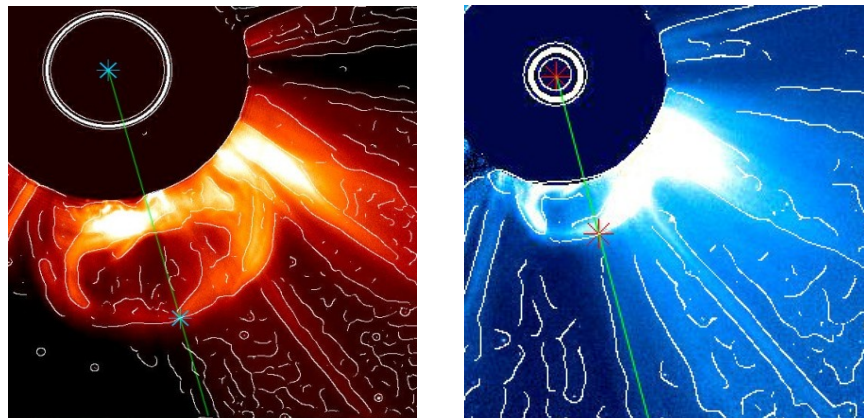


**Fig. 6.** Images prepared for further calculations, left: from LASCO C2 at 16:54 UT, right: from LASCO C3 at 17:42 UT on 18 April 2000. The straight lines show the selected direction along which the velocity of the CME front will be evaluated, this direction is determined by angle  $\alpha = 165^\circ$  measured clockwise from the vertical axis of the picture.

From Fig. 5 one can observe that the front edges obtained by Canny filter are thinner than presented in the paper <sup>4/</sup>. On every presented pictures the redundant/false edges are not removed manually.



The size of **one pixel** on the picture C2 is equal 11.9'' which conforms to the distance in space of about 8630 km, for the picture C3 the equivalent values are 56'' and 40500 km. These evaluations are the base of calculations of the propagation velocities of the CME leading edges. In the Table 1 they are shown for the CME on 18 April 2000: four pictures C2 and four C3. Symbols:  $\Delta t$  is the difference between the times of particular pictures, **h** is the high of the front edge above the in pixels, **H** is the same in Mkm,  $H/R_{Sun}$  is is the high of the front edge in solar radii, **v** velocity of the front edge.

**Table 1.** CME: 18 Apr 2000, start time 16:06, for angle  $\alpha = 165^\circ$

UT	$\Delta t$ [min]	h [pix]	H [Mkm]	V [km/sec]
16:06		268	2 313	
16:30	24	314	2 710	276
16:54	24	372	3 211	348
17:06	12	405	3 495	396
17:18	12	94	3 818	448
17:42	24	113	4 590	536
18:18	36	144	5 849	583
18:42	24	167	6 783	649

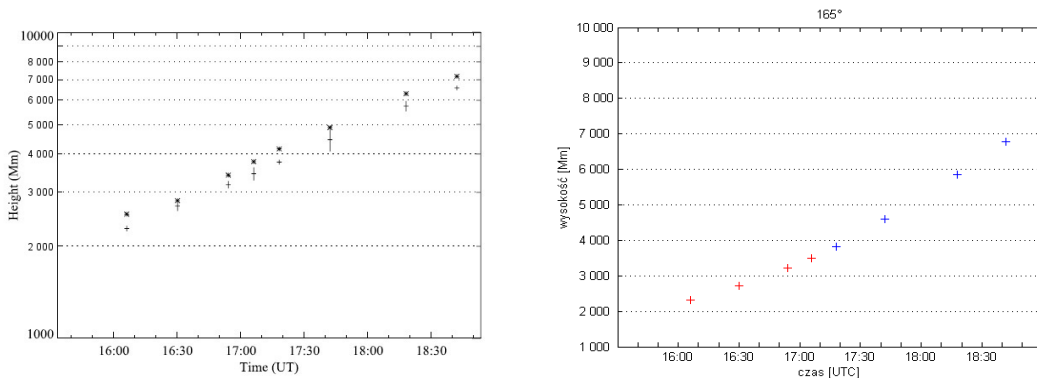


**Fig 7.** The height – time profiles for the 18 Apr 2000 CME. Left panel from Young and Gallagher <sup>4/</sup>, symbols: + data obtained via the multiscale method, \* data from CU CDAW CME catalog. Right panel. + data obtained from C2 images, + data calculated from C3 images. Errors are indicated by size of symbols +.

Fig. 7 shows the comparison of calculation of the velocities by 3 methods: manual, multiscale of Young and Gallagher, Canny's approach in this study. Generally speaking, for this

CME heights, and velocities, determined using standard/manual methods are larger by  $\approx 10\%$  than multiscale methods, and larger by 7-8% than Canny's method used here.

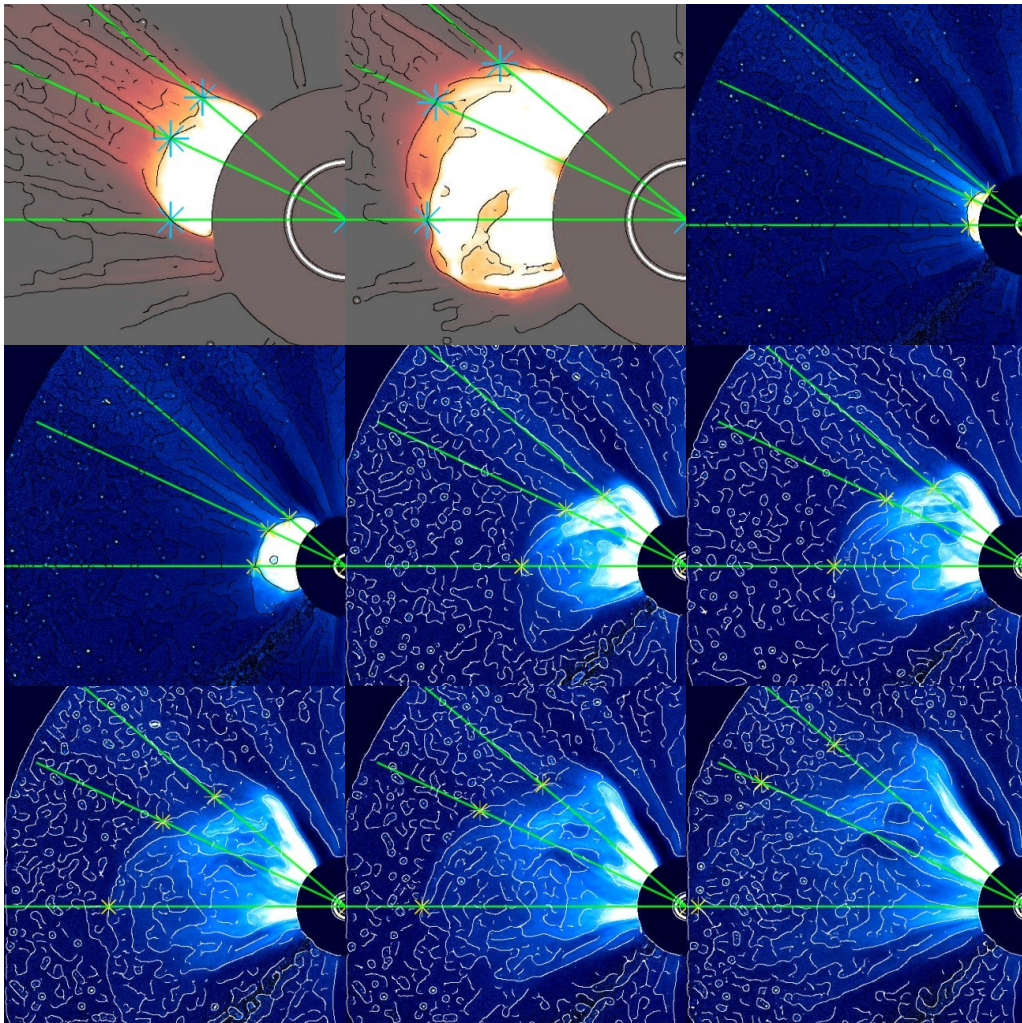


**Fig. 8.** LASCOCO C2 and C3 images of 1 Jun 2003 CME at 2:30 – 7:42 UT., chosen directions of propagation  $\alpha = 270^\circ / 295^\circ / 310^\circ$  are shown.

#### 4. CME: 1 June 2003

The data set contains two C2 images and seven C3 images. The C2 were taken using the orange filter (5400-6400 Å) with the variable cadence between 16 and 37 minutes and an image scale of 11.9 arcsec per pixel. The C3 s were taken using the clear filter (4000-8500 Å) with variable cadence between 24

**Table 2.** CME: 1 Jun 2003,  $\alpha = 270^\circ$ 

UT	$\Delta t$ [min]	h [pix]	H [Mkm]	V [km/sec]
02:30		243	2 097	
03:30	60	360	3 107	280
03:42	12	91	3 696	818
04:18	36	140	5 686	921
05:18	60	251	10 195	1252
05:42	24	294	11 941	1213
06:18	36	360	14 622	1241
06:42	24	402	16 327	1185
07:42	60	500	20 308	1106

**Table 3.** CME: 1 Jun 2003,  $\alpha = 295^\circ$ 

UT	$\Delta t$ [min]	h [pix]	H [Mkm]	V [km/sec]
02:30		268,0	2 313	
03:30	60	384,3	3 317	279
03:42	12	94,8	3 850	741
04:18	36	131,1	5 325	683
05:18	60	203,1	8 249	812
05:42	24	237,5	9 646	970
06:18	36	306,5	12 449	1297
06:42	24	346,3	14 065	1123
07:42	60	446,0	18 115	1125

**Table 4.** CME: 1 Jun 2003,  $\alpha = 310^\circ$ 

UT	$\Delta t$ [min]	h [pix]	H [Mkm]	V [km/sec]
02:30		261,7	2 259	
03:30	60	337,9	2 916	183
03:42	12	79,5	3 229	434
04:18	36	112,8	4 581	626
05:18	60	166,1	6 746	601
05:42	24	186,7	7 583	581
06:18	36	260,6	10 584	1390
06:42	24	286,7	11 644	736
07:42	60	383,3	15 568	1090

and 60 minutes and an image scale of 56 arcsec per pixel. Both C2 and C3 images were unpolarized. These images after preparation and treatment by Canny filter, as mentioned in Sec. 3, are shown on Fig. 8.

The determination of leading edges of CMEs facilitates calculation of velocity and acceleration of the hot plasma into

interplanetary space. On the Fig 8 and in the Tables 2 – 4, as e.g., the chosen directions are marked.

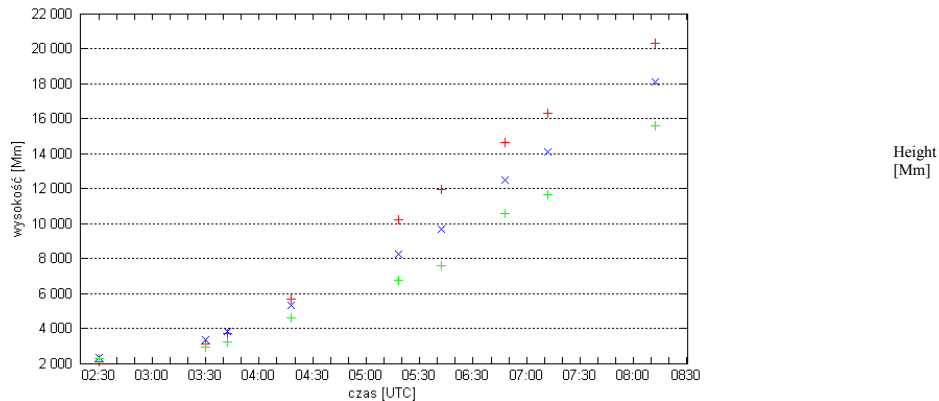


**Fig 9.** The height – time profiles for the 1 Jun 2003 CME. Symbols: + for  $\alpha = 270^\circ$ , x for  $\alpha = 295^\circ$ , + for  $\alpha = 310^\circ$  Errors are indicated by size of symbols +.

## 5. Conclusion

Canny's method is very successful in such tasks. This procedure should be developed in order to prepare fully automatic detection of CME leading edges.

## References

- [1] Gonzalez R., Woods R. Digital Image Processing, 3<sup>rd</sup> ed. Prentice-Hall, New Jersey, 2008.
- [2] //cdaw.gsfc.nasa.gov
- [3] Gallagher P.T., Lawrence G.R., Dennis B.R. *Astrophys. J.* **588**, L53-56, 2003.
- [4] Young C.A., Gallagher P.T. *Solar Phys.* **248**, pp. 457-469, 2008.
- [5] Stenborg G., Cobelli P.J. *Astron. Astrophys.* **398**, pp. 1185-1193, 2003.
- [6] Portier-Fozzani F., Vandame B., Bijaoui A., Maucherat A.J. *Solar Phys.* **201**, pp. 271-287, 2001.
- [7] <http://sidc.oma.be/cactus/>
- [8] Robbrecht E., Berghmans D. *Astron. Astrophys.* **425**, pp. 1097-1106, 2004.
- [9] Jung M. M.Sc dissertation supervised by Z. Kobylinski. Polish Air Force Academy, Deblin, Poland, 2014. (in Polish)
- [10] Roberts L.G. In: *Optical and Electro-Optical Information Proc.*, ed. by Tippet J.T. MIT Press Cambridge, Mass., 1965
- [11] Sobel I.E. *Camera Models in Machine Perception*, PhD thesis, Stanf. Univ. Press, N.Y., 1970.
- [12] Prewitt M.S. In: *Picture Processing and Psychopictorics*, eds. by Lipkin B.S., Rosenfeld A. Academic Press, N.Y., 1970.
- [13] Marr D., Hildreth E. *Proc. R. Soc. Lond.* **B207**, pp. 187-217, 1980.
- [14] Canny, J. A. *IEEE Trans. Pattern Analysis and Machine Intelligence*, **8(6)**, pp.679-698, 1986.
- [15] [sohodata.nascom.nasa.gov/cgi-bin/data\\_query](http://sohodata.nascom.nasa.gov/cgi-bin/data_query)
- [16] <http://www.gimp.org>

